

## Electrochemical Behavior of $\text{Li}_4\text{Ti}_5\text{O}_{12}$ /CNT Composite for Energy Storage

Hong-Il Kim, Jeong-Jin Yang, Han-Joo Kim, Tetsuya Osaka<sup>†</sup>, and Soo-Gil Park\*

Dept. of Industrial Engineering Chemistry, Chungbuk National University, 410 Seongbong-ro, Heungdeok-ku, Cheong-ju 361-763, Korea

<sup>†</sup>Graduate School of Science and Engineering, Waseda University, 3-4-1 Ohkubo, Shinjuku-ku 169-8555, Tokyo, Japan

(Received January 29, 2010 : Accepted February 17, 2010)

**Abstract :** The  $\text{Li}_4\text{Ti}_5\text{O}_{12}$ /CNT composite is prepared by ultrasound associated sol-gel method. The prepared composite is characterized by SEM, TEM, XRD and TG analysis, and their electrochemical behaviors are investigated by cyclic voltammetry, electrochemical impedance spectroscopy and charge-discharge test in 1M  $\text{LiBF}_4/\text{PC}$  electrolyte. From the results, it is identified that the  $\text{Li}_4\text{Ti}_5\text{O}_{12}$  nanoparticles coated on CNT surface have regular size with around 10~30 nm and spinel-framework structure. At the current rate of 20C, the discharge capacities of  $\text{Li}_4\text{Ti}_5\text{O}_{12}$ /CNT composites with CNT contents of 15, 30 and 50 wt% are 57, 63 and 48  $\text{mAhg}^{-1}$ , respectively, which have similar value. The improved electrochemical behavior of the  $\text{Li}_4\text{Ti}_5\text{O}_{12}$ /CNT composite electrode is attributed to the addition of CNT with electronic conductivity.

**Keywords :** Lithium titanium oxide, CNT, Composite, Conductivity

### 1. Introduction

The spinel  $\text{Li}_4\text{Ti}_5\text{O}_{12}$  is one of the most promising anode materials for high-power batteries or hybrid capacitors because it has an excellent Li-ion mobility and exhibits no structural change (zero-strain insertion material) during charge-discharge cycling.<sup>1-4)</sup> This material has a theoretical specific capacity of  $175 \text{mAhg}^{-1}$  and exhibits a practical specific capacity as high as  $160 \text{mAhg}^{-1}$  after 100 cycles.<sup>5,6)</sup> The flat charge and discharge curve of  $\text{Li}_4\text{Ti}_5\text{O}_{12}$  based materials show intercalation-deintercalation which takes place at around 1.5 V vs. Li. However, spinel  $\text{Li}_4\text{Ti}_5\text{O}_{12}$  has characteristics of initial capacity loss and poor rate capability due to the low electronic conductivity.<sup>7,8)</sup> The spinel  $\text{Li}_4\text{Ti}_5\text{O}_{12}$  used for high performance materials need to maintain capacities as current rates are increased.

To overcome this problem, several research have focused on improving its properties such as synthesis of nanoparticle size or spherical particle,<sup>9-12)</sup> substitution

of other metals or metal oxides,<sup>13,14)</sup> and composite with conductive carbons.<sup>7,8,15)</sup> Especially, conductive carbons based on  $\text{Li}_4\text{Ti}_5\text{O}_{12}$  composite improved its electrochemical behavior greatly with high rate and electronic conductivity. The combination material with carbon and  $\text{Li}_4\text{Ti}_5\text{O}_{12}$  has been commonly used as electrode materials but no previous work has been reported the influence of weight ratio between  $\text{Li}_4\text{Ti}_5\text{O}_{12}$  and carbon for high power lithium ion batteries or capacitors. In this work, we use composite materials from nano sized  $\text{Li}_4\text{Ti}_5\text{O}_{12}$  and carbon nanotube (CNT) and its electrochemical behaviors have been investigated with different contents.

### 2. Experimental

The  $\text{Li}_4\text{Ti}_5\text{O}_{12}$ /CNT composite was prepared by ultrasound associated sol-gel method. Stoichiometric amount of lithium hydroxide (LiOH, Reagent grade, = 98%, powder) and titanium isopropoxide ( $\text{Ti}[\text{OCH}(\text{CH}_3)_2]_4$ , 99.0%) at mole ratio of Li : Ti = 4.5 : 5 were dissolved in 2-methoxy ethanol ( $\text{CH}_3\text{OCH}_2\text{CH}_2\text{OH}$ , 99.0%), respectively. This mixed solution was magnetically stirred for 1 h at room temperature. Carbon nanotube (CNT,

\*E-mail: sgpark@chungbuk.ac.kr

multi-wall type, Hanwha Nanotech Co., Ltd.) dispersed in 2-methoxy ethanol with different weight ratio was added to mixture solution. The average outer diameter of CNT is 15~20 nm and the length is 10~20  $\mu\text{m}$ . The solution was stirred with 0.5 wt% PVP (poly vinyl pyrrolidone) as dispersant under ultrasound for 4 h. After then sol solution was dried to powders at 80°C for 10 h in air atmosphere and the powders were grounded in a zirconium mortar. The obtained powders were calcinated at 850°C for 5 h in argon atmosphere. Finally,  $\text{Li}_4\text{Ti}_5\text{O}_{12}/\text{CNT}$  composite was obtained. The crystal structure of the composite was characterized by X-ray diffraction using XDS 2000 (Sintag) model with Cu  $\alpha$  radiation source. The morphologies of composite materials were observed by a scanning electron microscopy (SEM, Hitachi S-2500C) and transmission electron microscope (TEM, Carl Zeiss Libra 120). Amount of CNT in composite was identified by thermo-gravimetry (TG, TA Instruments SDT 2960) analysis with heating rate of  $3\text{min}^{-1}$  from 30 to 900 in air atmosphere.

The electrodes were made of  $\text{Li}_4\text{Ti}_5\text{O}_{12}$  and  $\text{Li}_4\text{Ti}_5\text{O}_{12}/\text{CNT}$  composite (80 wt%) as an active material, carbon black (10 wt%) as an electric conductor and CMC, SBR and PTFE (2 wt%, 4 wt% and 4 wt%) as a binder on a copper foil, respectively. Li disk was used as the counter and reference electrodes. Then this electrode was dried at vacuum at 120°C for 24 h. It was fabricated for coin cell CR2016 model to measure electrochemical behaviors in 1 M  $\text{LiBF}_4/\text{PC}$  electrolyte. And the electrochemical behaviors were investigated by using cyclic voltammetry, AC impedance spectroscopy (Iviumstat) and charge-discharge test (Wonatech, WBCS3000).

### 3. Results and Discussion

Fig. 1 presents SEM and TEM images of  $\text{Li}_4\text{Ti}_5\text{O}_{12}/\text{CNT}$  composite. Fig. 1(a) shows the surface morphology of  $\text{Li}_4\text{Ti}_5\text{O}_{12}/\text{CNT}$  composite. As it shows, CNT had a part of straight form with thick outer diameter and  $\text{Li}_4\text{Ti}_5\text{O}_{12}$  nanoparticles are partly-aggregated on the surface of CNT. TEM image in Fig. 1(b) shows that  $\text{Li}_4\text{Ti}_5\text{O}_{12}$  particles had regular size with around 10~30 nm.

Fig. 2 shows the X-ray diffraction (XRD) patterns of  $\text{Li}_4\text{Ti}_5\text{O}_{12}$  and  $\text{Li}_4\text{Ti}_5\text{O}_{12}/\text{CNT}$  composite. The peaks located at 25.7° and 42.5° could be identified to the reflection from the (002) and (100) planes of CNT and the additional peaks observed at 18.4°, 35.6°, 37.3°, 44.3°, 47.3°, 57.2°, 62.8°, 66.1°, 74.3°, 75.3° and 79.3°

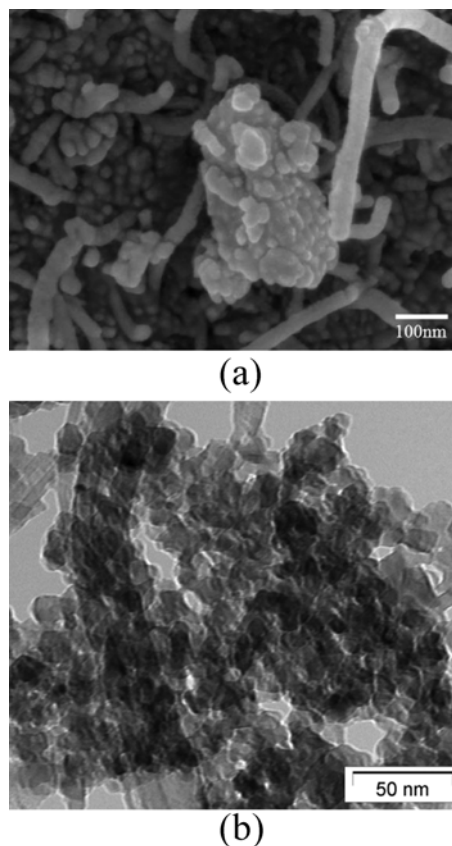


Fig. 1. (a) SEM images and (b) TEM images of  $\text{Li}_4\text{Ti}_5\text{O}_{12}/\text{CNT}$  (15 wt%) composite.

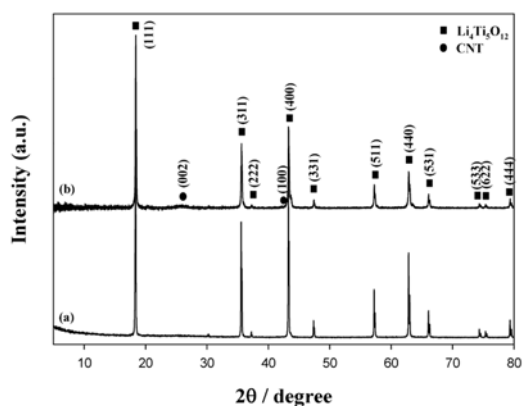


Fig. 2. X-ray diffraction patterns (Cu  $\text{K}\alpha$ ) of pristine  $\text{Li}_4\text{Ti}_5\text{O}_{12}$  (a) and  $\text{Li}_4\text{Ti}_5\text{O}_{12}/\text{CNT}$  (15 wt%) composite (b).

are corresponding to (111), (311), (222), (400), (331), (511), (440), (531), (533), (622) and (444) planes of spinel structure  $\text{Li}_4\text{Ti}_5\text{O}_{12}$  (JCPDS no. 21-1272). A broaden and

weaken peaks imply that  $\text{Li}_4\text{Ti}_5\text{O}_{12}/\text{CNT}$  composite belong to low-dimensional state. No peak of other phases was observed, which indicates that the composite are well crystallized.

Fig. 3 shows the TG curve of  $\text{Li}_4\text{Ti}_5\text{O}_{12}/\text{CNT}$  composite with a heating rate of  $3\text{min}^{-1}$  from room temperature to  $900^\circ\text{C}$  in air atmosphere. From the result,  $\text{Li}_4\text{Ti}_5\text{O}_{12}/\text{CNT}$  composite exhibit 15, 30 and 50 wt% of CNT contents, respectively. No weight loss or reaction was observed above  $600^\circ\text{C}$  on the curves, indicating that at the sintering temperature of  $850^\circ\text{C}$  pure phase  $\text{Li}_4\text{Ti}_5\text{O}_{12}$  nanoparticle can be formed. From above results, that the  $\text{Li}_4\text{Ti}_5\text{O}_{12}$  nanoparticles composited on the surface of CNT were successfully confirmed.

Fig. 4 shows the cyclic voltammogram obtained in the potential range of 0.8 to 2.5 V vs. Li disk as a refer-

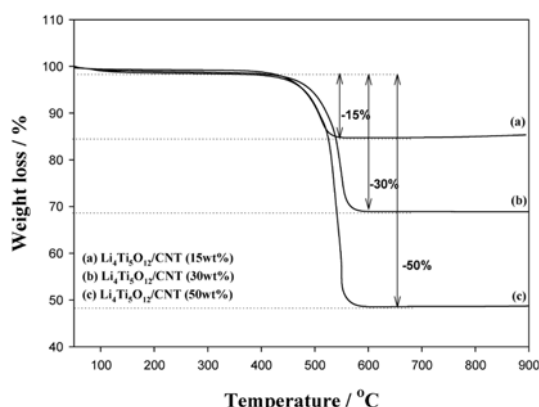


Fig. 3. TG curves of  $\text{Li}_4\text{Ti}_5\text{O}_{12}/\text{CNT}$  composite with CNT contents at air atmosphere. Temperature range:  $30\text{--}900^\circ\text{C}$ ,  $3\text{min}^{-1}$ .

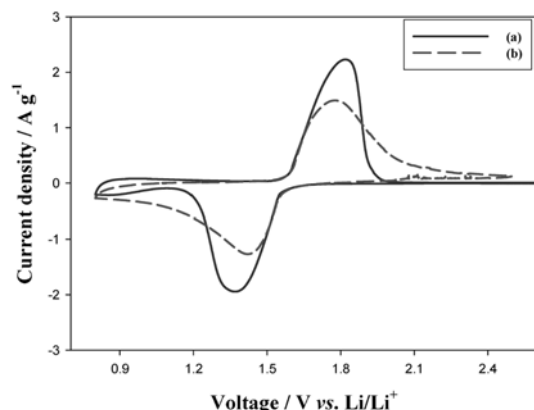


Fig. 4. Cyclic voltammograms of  $\text{Li}_4\text{Ti}_5\text{O}_{12}$  (a) and  $\text{Li}_4\text{Ti}_5\text{O}_{12}/\text{CNT}$  (15 wt%) composite electrode (b) at  $1\text{mVs}^{-1}$  in  $1\text{M LiBF}_4/\text{PC}$  electrolyte.

ence electrode. In the voltammograms of the  $\text{Li}_4\text{Ti}_5\text{O}_{12}$  and  $\text{Li}_4\text{Ti}_5\text{O}_{12}/\text{CNT}$  composite electrode, couples of reversible redox peaks at  $1.8\text{V}/1.45\text{V}$  were observed in  $1\text{M LiBF}_4/\text{PC}$  electrolyte at a scan rate of  $1\text{mVs}^{-1}$ , respectively. Any irreversible peak was not observed in the potential range of 0.8 to 2.5 V. The couple of peaks at  $1.8\text{V}/1.45\text{V}$  were attributed to the redox reaction of  $\text{Ti}^{4+}/\text{Ti}^{3+}$ .<sup>15)</sup> When  $\text{Li}_4\text{Ti}_5\text{O}_{12}$  nanoparticles were deposited on CNT, current density of  $\text{Li}_4\text{Ti}_5\text{O}_{12}/\text{CNT}$  composite electrode was slightly decreased than pristine  $\text{Li}_4\text{Ti}_5\text{O}_{12}$  particle with decreasing  $\text{Li}_4\text{Ti}_5\text{O}_{12}$  contents.

Fig. 5 shows Nyquist plots of the  $\text{Li}_4\text{Ti}_5\text{O}_{12}/\text{CNT}$  composite electrodes in the frequency range 100 kHz to 10 mHz with CNT contents at the voltage of 1.56, respectively. The plot is composed of a semicircle at high frequency and an oblique straight line at low frequency. The resistance  $R_s$ , which corresponds to the electrolyte resistance, was decreased with increasing CNT contents. The semicircle reflects the electrochemical reaction resistance and the double layer capacity of the electrode. The comparing with pristine  $\text{Li}_4\text{Ti}_5\text{O}_{12}$  electrode, charge-transfer resistances  $R_{ct}$  of  $\text{Li}_4\text{Ti}_5\text{O}_{12}/\text{CNT}$  composite electrodes were decreased respectively with increasing CNT contents.

Fig. 6 shows the charge-discharge curves for the  $\text{Li}_4\text{Ti}_5\text{O}_{12}/\text{CNT}$  composite electrode at a current density of 1C at cut-off voltages 2.5~0.8 V. It clearly shows a curved line with lithium insertion reaction. Its reaction follows below.<sup>16)</sup>

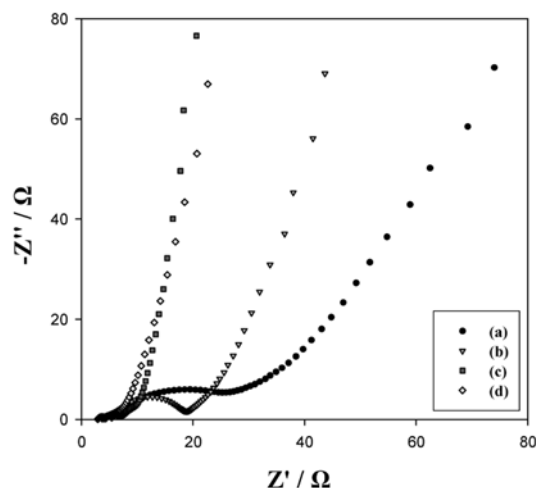


Fig. 5. Nyquist plots of  $\text{Li}_4\text{Ti}_5\text{O}_{12}$  (a),  $\text{Li}_4\text{Ti}_5\text{O}_{12}/\text{CNT}$  (15 wt%) (b),  $\text{Li}_4\text{Ti}_5\text{O}_{12}/\text{CNT}$  (30wt%) (c) and  $\text{Li}_4\text{Ti}_5\text{O}_{12}/\text{CNT}$  (50 wt%) (d) composite in  $1\text{M LiBF}_4/\text{PC}$  electrolyte. Frequency range :  $100\text{kHz}\text{--}10\text{mHz}$ .

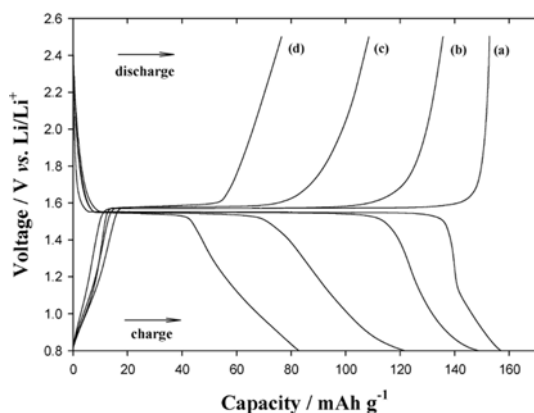
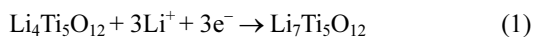


Fig. 6. Charge and discharge curves of  $\text{Li}_4\text{Ti}_5\text{O}_{12}$  (a),  $\text{Li}_4\text{Ti}_5\text{O}_{12}/\text{CNT}$  (15 wt%) (b),  $\text{Li}_4\text{Ti}_5\text{O}_{12}/\text{CNT}$  (30 wt%) (c) and  $\text{Li}_4\text{Ti}_5\text{O}_{12}/\text{CNT}$  (50 wt%) (d) composite at 1C in 1 M  $\text{LiBF}_4/\text{PC}$  electrolyte.



The discharge capacity of the  $\text{Li}_4\text{Ti}_5\text{O}_{12}$  electrode was similar to theoretical capacity of  $\text{Li}_4\text{Ti}_5\text{O}_{12}$ . When CNT content of  $\text{Li}_4\text{Ti}_5\text{O}_{12}/\text{CNT}$  composite electrode was increased, discharge capacity of  $\text{Li}_4\text{Ti}_5\text{O}_{12}/\text{CNT}$  composite electrode was decreased from  $152 \text{ mAhg}^{-1}$  ( $\text{Li}_4\text{Ti}_5\text{O}_{12}$ ) to  $77 \text{ mAhg}^{-1}$  ( $\text{Li}_4\text{Ti}_5\text{O}_{12}$ -50 wt%). When  $\text{Li}_4\text{Ti}_5\text{O}_{12}$  contents was decreased, specific capacity of  $\text{Li}_4\text{Ti}_5\text{O}_{12}/\text{CNT}$  composite electrode was decreased. The calculated  $\text{Li}_4\text{Ti}_5\text{O}_{12}$ 's capacities based on  $\text{Li}_4\text{Ti}_5\text{O}_{12}$  contents vs.  $\text{Li}_4\text{Ti}_5\text{O}_{12}/\text{CNT}$  composite entire weight were shown (a) line in Fig. 7. The  $\text{Li}_4\text{Ti}_5\text{O}_{12}/\text{CNT}$ 's discharge specific capacity is very close to theoretical capacity of  $\text{Li}_4\text{Ti}_5\text{O}_{12}$  ( $175 \text{ mAhg}^{-1}$ ). It showed that  $\text{Li}_4\text{Ti}_5\text{O}_{12}$  nanoparticle had reversible capacity. Generally, the large irreversible capacity of CNT is attributed to electrolyte reduction and formation of a solid electrolyte interface (SEI) layer on the carbon surface. But the irreversible capacity of  $\text{Li}_4\text{Ti}_5\text{O}_{12}/\text{CNT}$  is relatively lower than that of CNT since the  $\text{Li}_4\text{Ti}_5\text{O}_{12}$  suppress the formation of surface films.

Fig. 8 shows the discharge capacity of  $\text{Li}_4\text{Ti}_5\text{O}_{12}/\text{CNT}$  composite electrode during cycling at different current rates in the voltage range of 2.5~0.8 V. At increasing current rate, capacity of composite electrode was gradually decreased, but when the relative contents of CNT was increased on  $\text{Li}_4\text{Ti}_5\text{O}_{12}/\text{CNT}$  composite the capacities loss of composite were decreased. At the current rate of 20C, the discharge capacities of CNT contents with 15, 30 and 50 wt% are 57, 63 and  $48 \text{ mAhg}^{-1}$ ,

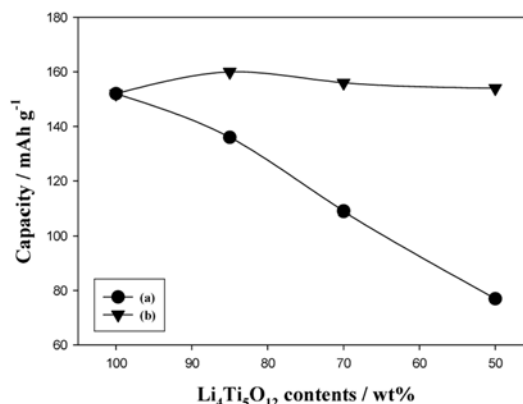


Fig. 7. Capacity dependence of  $\text{Li}_4\text{Ti}_5\text{O}_{12}/\text{CNT}$  composite entire weight (a) vs.  $\text{Li}_4\text{Ti}_5\text{O}_{12}$  contents (b).

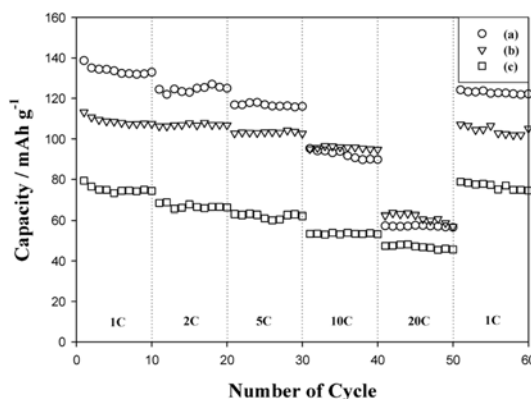


Fig. 8. Cycle performance of  $\text{Li}_4\text{Ti}_5\text{O}_{12}/\text{CNT}$  (15 wt%) (a),  $\text{Li}_4\text{Ti}_5\text{O}_{12}/\text{CNT}$  (30 wt%) (b) and  $\text{Li}_4\text{Ti}_5\text{O}_{12}/\text{CNT}$  (50 wt%) (c) composite with different current rate.

respectively, which have similar value with each other. It was attributed to electronic conductivity's enhancement of  $\text{Li}_4\text{Ti}_5\text{O}_{12}/\text{CNT}$  composite electrode by increasing CNT contents. As the result, we were identified that the electrochemical behavior of  $\text{Li}_4\text{Ti}_5\text{O}_{12}/\text{CNT}$  composite electrode was improved.

#### 4. Conclusion

The  $\text{Li}_4\text{Ti}_5\text{O}_{12}/\text{CNT}$  composite was prepared by ultrasound associated sol-gel method. We were identified that the  $\text{Li}_4\text{Ti}_5\text{O}_{12}$  nanoparticles had regular size with around 10~30 nm and showed spinel-framework structure. At increasing current rate, capacity of composite electrode was gradually decreased but at increasing CNT contents, capacities losses were decreased. The im-

proved electrochemical behavior of the  $\text{Li}_4\text{Ti}_5\text{O}_{12}/\text{CNT}$  composite electrode was attributed to the addition of CNT with electronic conductivity. The synthesized  $\text{Li}_4\text{Ti}_5\text{O}_{12}/\text{CNT}$  composite electrode shows a promising candidate for electrode materials used in high power lithium ion batteries or capacitors.

### Acknowledgement

This work is the outcome of a Manpower Development Program for Energy & Resources and the Chungbuk Local Industrial Tech. & Development Project(No. 70006864) supported by the Ministry of Knowledge and Economy.

### References

1. L. Cheng, H. J. Liu, J. J. Zhang, H. M. Xiong, and Y. Y. Xia, 'Nanosized  $\text{Li}_4\text{Ti}_5\text{O}_{12}$  prepared by molten salt method as an electrode material for hybrid electrochemical supercapacitors' *J. Electrochem. Soc.*, **153**, A1472 (2006).
2. K. Ariyoshi, S. Yamamoto, and T. Ohzuku, 'Three-volt lithium-ion battery with  $\text{Li}[\text{Ni}_{1/2}\text{Mn}_{3/2}]\text{O}_4$  and the zero-strain insertion material of  $\text{Li}[\text{Li}_{1/3}\text{Ti}_{5/3}]\text{O}_4$ ' *J. Power Sources*, **119-121**, 959 (2003).
3. T. Ohzuku, A. Ueda, and N. Yamamoto, 'Zero-Strain Insertion Material of  $\text{Li}[\text{Li}_{1/3}\text{Ti}_{5/3}]\text{O}_4$  for Rechargeable Lithium Cells' *J. Electrochem. Soc.*, **142**, 1431 (1995).
4. A. D. Pasquier, A. Laforgue, and P. Simon, ' $\text{Li}_4\text{Ti}_5\text{O}_{12}/\text{poly}(\text{methyl})\text{thiophene}$  asymmetric hybrid electrochemical device' *J. Power Sources*, **125**, 95 (2004).
5. K. Nakahara, R. Nakajima, T. Matsushima, and H. Majima, 'Preparation of particulate  $\text{Li}_4\text{Ti}_5\text{O}_{12}$  having excellent characteristics as an electrode active material for power storage cells' *J. Power Sources*, **117**, 131 (2003).
6. Y. Bai, F. Wang, F. Wu, C. Wu, and L. Bao, 'Influence of composite  $\text{LiCl-KCl}$  molten salt on microstructure and electrochemical performance of spinel  $\text{Li}_4\text{Ti}_5\text{O}_{12}$ ' *Electrochim. Acta*, **54**, 322 (2008).
7. J. Huang and Z. Jiang, 'The preparation and characterization of  $\text{Li}_4\text{Ti}_5\text{O}_{12}/\text{carbon nano-tubes}$  for lithium ion battery' *Electrochim. Acta*, **53**, 7756 (2008).
8. J. Gao, J. Ying, C. Jiang, and C. Wan, 'High-density spherical  $\text{Li}_4\text{Ti}_5\text{O}_{12}/\text{C}$  anode material with good rate capability for lithium ion batteries' *J. Power Sources*, **166**, 255 (2007).
9. A. Guerfi, S. Sévigny, M. Lagacé, P. Hovington, K. Kinoshita, and K. Zaghib, 'Nano-particle  $\text{Li}_4\text{Ti}_5\text{O}_{12}$  spinel as electrode for electrochemical generators' *J. Power Sources*, **119-121**, 88 (2003).
10. M. Venkateswarlu, C. H. Chen, J. S. Do, C. W. Lin, T. C. Chou, and B. J. Hwang, 'Electrochemical properties of nano-sized  $\text{Li}_4\text{Ti}_5\text{O}_{12}$  powders synthesized by a sol-gel process and characterized by X-ray absorption spectroscopy' *J. Power Sources*, **146**, 204 (2005).
11. J. Gao, C. Jiang, J. Ying, and C. Wan, 'Preparation and characterization of high-density spherical  $\text{Li}_4\text{Ti}_5\text{O}_{12}$  anode material for lithium secondary batteries' *J. Power Sources*, **155**, 364 (2006).
12. K. Kanamura, T. Chiba, and K. Dokko, 'Preparation of  $\text{Li}_4\text{Ti}_5\text{O}_{12}$  spherical particles for rechargeable lithium batteries' *J. Eur. Ceram. Soc.*, **26**, 577 (2006).
13. K. Mukai, K. Ariyoshi, and T. Ohzuku, 'Comparative study of  $\text{Li}[\text{CrTi}]\text{O}_4$ ,  $\text{Li}[\text{Li}_{1/3}\text{Ti}_{5/3}]\text{O}_4$  and  $\text{Li}_{1/2}\text{Fe}_{1/2}[\text{Li}_{1/2}\text{Fe}_{1/2}\text{Ti}]\text{O}_4$  in non-aqueous lithium cells' *J. Power Sources*, **146**, 213 (2005).
14. S. Huang, Z. Wen, J. Zhang, and X. Yang, 'Improving the electrochemical performance of  $\text{Li}_4\text{Ti}_5\text{O}_{12}/\text{Ag}$  composite by an electroless deposition method' *Electrochim. Acta*, **52**, 3704 (2007).
15. H. Ge, N. Li, D. Li, C. Dai, and D. Wang, 'Electrochemical characteristics of spinel  $\text{Li}_4\text{Ti}_5\text{O}_{12}$  discharged to 0.01 V' *Electrochem. Commun.*, **10**, 719 (2008).
16. J. L. Allen, T. R. Jow, and J. Wolfenstine, 'Low temperature performance of nanophase  $\text{Li}_4\text{Ti}_5\text{O}_{12}$ ' *J. of Power Sources*, **159**, 1340 (2006).